이학석사 학위논문

# Catalyst-free growth of graphene, hexagonal boron nitride and their heterostructures

## 비촉매 성장법을 이용한 그래핀, 질화붕소와 이종구조 합성

2017년 2월

서울대학교 대학원

물리천문학부 물리학 전공

윤 지 영

# Abstract

Graphene and hexagonal boron nitrde(hBN) vertical heterostructure was grown using catalyst-free chemical vapor deposition techinique. Graphene and hBN were grown on hBN and graphene respectively, and graphene/hBN and hBN/graphene structures were obtained. The effect of growth conditions has been studied. The films were characterized with FE-SEM, Raman spectroscopy and TEM. Graphene islands or 3-dimensional nanostructure were grown on hBN flakes depending on the growth conditions. G-peak and 2D-peak were shown on the Raman spectrum obtained from the graphene grown hBN flakes. hBN film or 3-dimensional nanostructures were grown on exfoliate graphite and CVD graphene layers. The morphology was changed from film to 3-dimensional nanorods depending on the growth conditions. On the Raman spectrum, hBN peak was observed in addition to graphene peaks. Based on the growth conditions developed for Graphene/hBN and hBN/graphene growth structures, hBN / graphene / hBN vertical heterostructure was attempted to be grown by sequential growth of graphene and hBN on hbN flake. The growth of film was confirmed with FE-SEM and Raman spectroscopy. Analyzing microstructure with HR-TEM, The lattice constant of film covering the surface was same with hBN and Moire pattern was observed from the film grown on hBN flake.

**Keyword** : catalyst-free CVD, graphene, hBN, heterostructures
**Student Number** : 2015-20341

# Table of contents

**Abstract** .....

**Table of contents** ..... i

**List of figures** ..... v

**List of tables** ..... vii

**Chapter 1. Introduction** ..... 1

**Chapter 2. Literature** ..... 4

2.1. Catalyst assisted CVD growth of graphene, hBN and their heterostructures ..... 4

2.2. Catalyst-free CVD growth of graphene and hBN ..... 5

**Chapter 3. Experiments** ..... 7

3.1. CVD setup ..... 7

3.2. Structural characterization ..... 10

3.3. Optical characterization ..... 10

**Chapter 4. hBN growth on graphite and graphene layers** ..... 12

4.1. Effect of temperature on hBN growth ..... 12

4.2. Effect of pressure on hBN growth ..... 17

4.3. Effect of borazine flowrate on hBN growth ..... 21

4.4. Effect of growth time on hBN growth ..... 24

4.5. Summary ..... 27
**Chapter 5. Graphene growth on hBN layers ..... 28**
5.1. Effect of pressure on graphene growth ..... 28
5.2. Effect of temperature on graphene growth ..... 32
5.3. Effect of ethylene flowrate on graphene growth ..... 34
5.4. Summary ..... 36
**Chapter 6. Sequential growth of hBN and graphene on hBN layers ..... 37**
6.1. Sequential growth of graphene and hBN ..... 37
6.2. FE-SEM images and Raman spectrum of the film ..... 39
6.3. Microstructure of hBN/graphene grown on hBN flakes ..... 42
6.4. Summary ..... 44
**Chapter 7. Conclusion ..... 45**
7.1. Summary ..... 45
**Reference ..... 46**
**Summary in Korean ..... 50**

# List of figures

Figure3.1. Gas delivery system for CVD setup..... 9

Figure3.2. Schematic illustration for the micro-Raman measurement ..... 11

Figure 4.1. FE-SEM images of hBN film grown on various graphene layers with different growth temperature. hBN grown at (a-c) 1150'C, (d-f) 1100'C, (g-i) 1050'C. ..... 15

Figure 4.2. Raman spectra of hBN film grown on graphene layers. Raman spectrum of hBN grown on (a) CVD multi-layer graphene and (b) graphite flake with $O_2$ plasma treatment. (c, d) the magnified spectrum of (a) and (b)..... 16

Figure 4.3. FE-SEM images of hBN film grown on various graphene layers with pressure. hBN grown at (a-c) 150 torr, (d-f) around 300 torr, and (g-i) around 650 torr..... 19

Figure 4.4. Raman spectra of hBN film grown on graphene layers. hBN film grown on (a) CVD multi-layer graphene and (b) graphite flake with O2 plasma treatment. (c, d) the magnified Raman spectra of (a) and (b)..... 20

Figure 4.5. FE-SEM images of hBN film grown on various graphene layers with different borazine flowrate. hBN grown with (a-b) 6 sccm, (c-d) 8 sccm, and (e-f) 10 sccm of borazine flowrate. ..... 23

Figure 4.6. FE-SEM images of hBN film grown on various graphene layers with different growth time. hBN grown for (a-b) 15 minutes, (c-d) 30 minutes, and (e-f) 60 minutes. ..... 26

Figure 5.1. FE-SEM images of graphene islands grown on hBN flakes with different pressure and growth time. graphene was grown for 10 minutes under (a) 50 torr, (b) 300 torr and (c) 740 torr. (d) Graphene was grown for

30 minutes under 740 torr..... 30
Figure 5.2. Raman spectra of graphene grown under different pressure and growth time. Black and red arrows indicates the Raman peaks of graphene and hBN respectively. To compare the spectra, intensity of spectra was normalized and vertically shifted..... 31
Figure 5.3. FE-SEM images and corresponding Raman spectra of graphene grown on hBN flakes with growth temperature. Graphene was grown at (a) 1000'C (b) 1100'C and (c) 1150'C. (d-f) corresponding Raman spectrum of graphene grown on hBN. ..... 33
Figure 5.4. FE-SEM images graphene grown on hBN flake with different ethylene flowrate. Graphene was grown with (a) 50 sccm ,(b) 100sccm (c) 150 sccm, and (d) 200 sccm of ethylene. The red arrows indicates the graphene islands with hexagonal shape ..... 35
Figure 6.1. Schematics of experiment. Sequential growth of graphene and hBN on hBN flakes..... 38
Figure 6.2. FE-SEM images of film after the sequential growth. a) On pristine hBN flake, b) On hBN flake oxidized under 900'C for 3 hours..... 41
Figure 6.3. Raman spectrum of the film after the sequential growth. Spectrum obtained from a) pristine hBN flake and b) oxidized hBN flake..... 41
Figure 6.4. High resolution TEM images of film grown on hBN flake after the sequential growth. a) High resolution TEM image and corresponding FFT image(inset) b) Low magnification TEM image showing Moire pattern..... 43

# List of tables

Table 3.1. growth conditions for graphene and hBN..... 9

# Introduction

# 1

After discovery of graphene, the researches about 2-dimensional materials(2D materials) which have atomic layered structures with each layer bonded with Van der waals force were flourished. Specifically about heterostructures, 2D materials were bonded with Van der waals force and can be stacked while maintaining the physical and electrical property of individual layer unlike the conventional semiconducting materials which have dangling bond on the surface and lattice mismatch inhibits the stacking of atomic layers, and it enables fabricating a new type of devices such as tunneling transistors. New type of devices show potential for 2D materials to be utilized for electronic devices beyond silicon technology and many researchers are focusing on the 2D materials.

Graphene consists of carbon atoms with hcp structure in single atomic layer. Lattice constants of graphene is known as a=2.46Å. The carbon atoms in each layers form $sp^2$ bonding with surrounding 3 carbon atoms and φ-bonding with adjacent layers. Because of the difference in bonding, the in-plane and out-of-plane properties of graphene are also different. Concerning the electrical properties, graphene is semi-metallic and known to have high mobility. Although it does not have band gap, the electrical, have fermi laver around the Dirac point in k-space, the density of state is very low when it is not doped. Hexagonal boron nitride(hBN) also have hexagonal closed packed structure with lattice constant a=2.5Å, having 0.2% of lattice mismatch comparing with graphene. hBN is known to have 5.7eV of bandgap, electrically insulating. hBN is chemically inert and stable under high

temperature. This properties highlight hBN as substrate or encapsulation layer for 2D materials.

Both graphene and hBN, having no band gap or too large band gap, are not proper material to be utilized as electronic devices which needs reasonable band structures. However the heterostructures of both material enabled by stacking atomically thin layers open a new prospects in the field of electronic device. Specifically, utilizing the atomically thin nature of 2D materials and stacking the heterostructures, tunneling transistor or band structure modulation has been realized, which was not possible with conventional semiconducting materials. Based on this observation many researchers are focusing on growing or fabricating heterostructure of 2D materials.

Although the growth of individual 2D materials were accomplished on metal catalyst, the growth of heterostructures were barely reported. The catalyst effect enables the growth of high quality 2D materials but only few-layered 2D material can be grown because of limited catalyst effect. Additionally, the growth of semiconducting materials on catalyst alters the catalytic property, growth behavior can even be changed when growing heterostructures. With this backgrounds, new approach was needed in fabricating the heterostructures or supperlattice of 2D materials.

In this research, catalyst-free chemical vapor deposition technique was adopted as a new technique for fabricating the heterostructures of 2D materials. Growth of graphene, hBN and their heterostructure have been demonstrated and the effect of growth conditions have been studied using

Cold-wall CVD setup. Based on the growth conditions developed for graphene and hBN growth, the growth of vertical heterostructures of graphene and hBN has been attempted by sequential growth of graphene and hBN.

# Literature

# 2

## 2.1. Catalyst assisted CVD growth of graphene, hBN and their heterostructures

The growth of high quality 2D materials and their heterostructure is very important research in commercializing and utilizing 2D materials as various type of devices. Although there are various growth techniques reported in growing large scale high quality 2D materials, it is known that CVD method using catalyst substrates reproduced the high quality 2D materials comparable to exfoliated graphene.[1] Since the first CVD growth of graphene was accomplished on copper foil, the graphene growth was done on various metal which can work as catalyst.[2-6] As the metal substrate enables the self-limited growth of 2D materials and layered growth, large-scale growth of uniform 2D material was also reported by several groups.[7-11] Same strategy was applied in growing hBN, it was grown on various metals and growth behaviors were investigated.[12-18]

However there were several drawbacks of growing 2D materials on metal catalyst. In order to utilize the 2D materials, it needs to be detached from the metal substrate and transferred to target substrates. PMMA assisted or polymer assisted transfer techniques were developed to transfer the 2D materials but the quality of 2D materials were degraded while the transfer process. For example, metal residues resided between the 2D materials and the substrate and it cannot be perfectly removed.[19] Polymer residue also remains on the surface of 2D

materials, decreases the mobility of graphene and making graphene doped.[20] Additionally, the transfer process can introduces tear off or wrinkles on 2D materials, also degrades the quality.[21] In addition to degrade of quality, the difficulties in fabricating heterostructures also inhibits the utilizing 2D materials grown on metal catalyst. When growing graphene and hBN vertical heterostructures on metal catalyst, the growth behavior changes depending on the underlying film. In case growing graphene on hBN covered copper foil, it was reported that the growth rate of graphene decreases with increasing the thickness of underlying hBN.[22] When growing hBN/graphene/hBN structures on copper, the growth behavior of hBN on graphene is different from the growth of 1$^{st}$ layer of hBN, implies that the graphene affects the catalytic effects of copper.[23]

## 2.2. Catalyst-free CVD growth of graphene and hBN

In order to avoid the problems in catalyst-assisted growth, catalyst-free growth techinique has been attempted on various substrate. Conventionally dielectric substrates, Silicon dioxide and sapphire, were firstly used in growing graphene but the quality of graphene is much poor comparing to that grown on metal catalyst.[24-26] It was reported that hBN which has negligible lattice mismatch with graphene can be used as substrate for epitaxial growth of graphene and have electrical property comparable to graphene grown on metal catalyst, opens up the growth of 2D heterostructures without metal catalyst.[27-32]

The growth of high quality hBN layer was reported mainly on conventional sapphire substrate which was occasionally used as substrate for the growth of 3-5 semiconductor materials. Several groups reported the growth of hBN on sapphire substrates using MOCVD method. Wafer-scale, epitaxial and

atomically flat hBN was achieved using similar CVD method under higher temperature comparing with catalyst-assisted growth.[33] The growth of hBN on graphene is barely reported. Lee reported the growth of atomically flat hBN on nanocrystalline graphene, utilizing catalytic effects of C-O bonding of nanocrystalline graphene[34]. They showed that the growth of atomically flat hBN on graphene is difficult because of lack of bondings between each layer. Cho reported the first growth of hBN on graphite layers using high temperature MBE[35]. They obtained few layer hBN on graphite layers and observed tunneling characteristics depending on the thickness of hBN layer.

# Experiments

# 3

## 3.1. CVD setup

This section describes the setup used for the graphene and hBN growth. The figure shows the schematic of CVD system for graphene and hBN growth. The setup can be classified in to 3 section, the gas delivery system, pressure control system, and the reaction chamber.

Ethylene was used as carbon source for the graphene growth and borazine was used as boron and nitrogen source for hBN growth. Liquid borazine was stored in bubbler and the temperature of bubbler was maintained at -15°C to control the amounts of vapor pressure of borazine constant. Using borazine, the pressure inside the bubbler and gas line was maintained to be higher than the pressure inside the chamber to prevent for gas to be flow backward. Nitrogen was used as carrier gas for borazine instead of hydrogen to prevent the chemical reactions while delivering gaseous borazine into the chamber. Hydrogen and ammonia were introduced into the chamber to control the chemical reaction required to grow graphene and hBN. The amounts of gas introduced into the chamber were precisely controlled with mass flow controllers and pneumatic valves.

The pressure inside the chamber was controlled with throttle valve controlled with pressure controller and the bypass line directly connected to the exhaust. When the experiment was carried out under low-pressure, under

atmospheric pressure, angle valve was open and the pressure was controlled with throttle valve. Pressure was measured with baratron gauge adapted to chamber and the throttle valve was consistently controlled to maintain the pressure constant. Rotary pump was used to exhaust the gas inside the chamber. When the experiment was done under atmospheric pressure, gas flew through a bypass line connected to the exhaust line.

Induction heating system was used to control the temperature of substrate. Graphite or SiC coated graphite susceptor were placed inside the chamber. Multiple coils surrounded the susceptor outside the chamber, and the magnetic field generated by the current flow induced the current on susceptor and heated susceptor. The thermocouple was positioned inside the susceptor through the hollow quartz stick supporting the susceptor. Based on the temperature measured by thermocouple, the power of induction heater was consistently controlled by temperature controller to maintain the temperature on the specific value. The substrates were loaded on the susceptor and the temperature of sample is expected to be similar to the temperature measured by thermocouple.

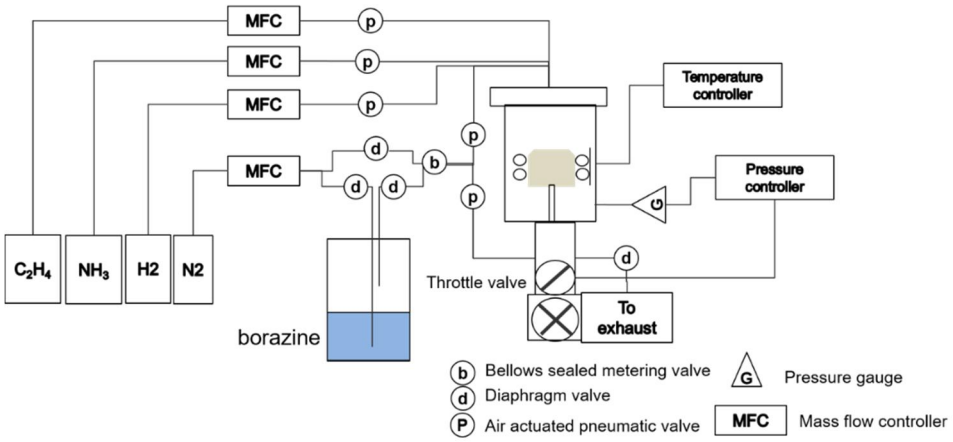


**Figure3.1. Gas delivery system for CVD setup**

**Table 3.1. growth conditions for graphene and hBN**

| | **Graphene** | **hBN** |
|---|---|---|
| Substrate temperauture (°C) | 1000 - 1200 (1150) | 1050 – 1150 (1150) |
| Growth time (min) | 10 – 30 (30) | 15 – 60 (30) |
| Reactor pressure (torr) | 50 - 750 (750) | 150 – 650 (650) |
| $H_2$ flowrate (sccm) | 2600 | 0 |
| N2 flowrate | 0 | 0 |
| $NH_3$ flowrate (sccm) | 0 | 2600 |
| Borazine flowrate (sccm) | 0 | 6-10 (8) |
| ( ) : preferable conditions | | |

## 3.2. Structural characterization

Surface morphology was investigated using TESCAN field-emission SEM (FE-SEM). Typical acceleration voltage and magnification were 30 kW and 30–500,000, respectively.

Microstructural characteristics were investiagated using high-resolution transmission electron microscopy (HR-TEM). The measurement was done by Hongweok Oh.

## 3.3. Optical characterization

For the characterization of graphene and hBN layers, micro-Raman spectroscopy was used. The excitation laser was focused on a sample using objective(x50), and the Raman signals from the sample were collected by the same objective and dispersed in a monochromator (Monora 320i, Dongwoo) equipped with thermoelectric cooled charge-coupled device (CCD) (DU401A-UV, Andor). The spot size of laser beam was smaller than 20 by 20 $\mu m^2$, enables obtaining Raman signals from small exfoliated flakes. A typical scan range was 1000~2900 $cm^{-1}$. Diode-pumped solid state (532 nm) was used as an excitation laser. Calibration was done using graphite and hBN flake, locating G-, 2D- and hBN peak at 1580$cm^{-1}$, 2700$cm^{-1}$ and 1367$cm^{-1}$ respectively.

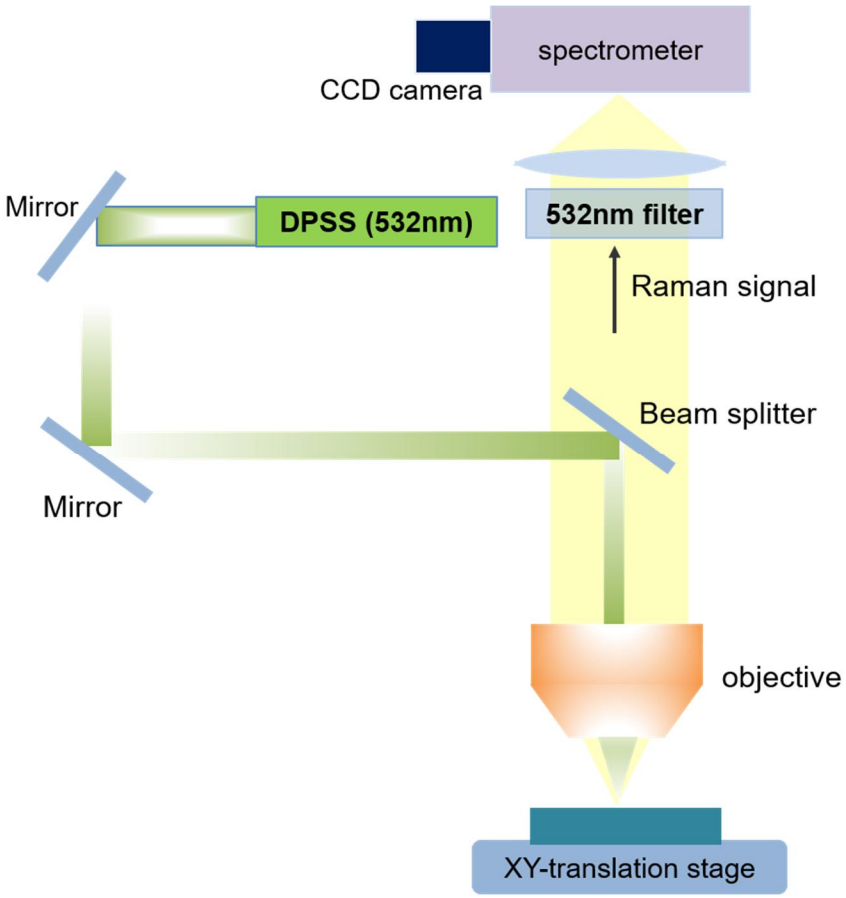


**Figure3.2. Schematic illustration for the micro-Raman measurement**

# hBN growth on graphite and graphene layers

# 4

This chapter describes the growth of hBN on graphite layers under various growth conditions. The growth of hBN on graphene layer was barely reported by other groups. Thus, effects of growth conditions were not even studied. In this chapter, growth of hBN has been conducted while varying the growth conditions—growth temperature, pressure, flowrate of borazine and growth time—and the effect of each parameter has been observed.

## 4.1. Effect of temperature on hBN growth

The effect of growth temperature has been studied. hBN films were grown at various temperatures of 1050 – 1150˚C. CVD graphene, graphite flake and graphite flake with $O_2$ plasma treatment were used as substrates.

Figure4.1. shows FE-SEM images of hBN film grown on graphene films. On CVD graphene, film-like feature was observed regardless of the growth temperature. At 1150˚C, flat film and nanostructure were grown on the substrate. CVD graphene layer was fully covered by the hBN film and nanoneedles and nano particles were grown on the film. The diameter of needle is about 100nm. At 1100˚C, still, flat film and nanostructure were grown on the substrate. The morphology of nanostructure was changed from nanoneedle to nanoparticle as the temperature decreased from 1150˚C to 1100˚C. Additionally, the density of the nanostructure was decreased

comparing with the sample grown at 1150'C. When temperature was further decreased to 1050'C, the density of nanostructure was significantly reduced and the film with different contrast was observed. In comparison with the hBN film grown with the higher temperature, film grown at 1050'C shows non-uniform contrast. Considering that the electrical conductivity affects the contrast of SEM images, bright and dark regions might be hBN and graphene respectively. It seems that the hBN film does not fully covers the graphene layers when the temperature was reduced.

On exfoliated graphite flake with $O_2$ plasma treatment, flat islands were observed. At 1150'C, 200~300nm size islands were grown with flat surface and the islands merged into one complete film. Unlike CVD graphene, nanostructures were barely observed and only nanoparticles are observed on the surface of the film. As the temperature decreases, the size of island seems to be decreased to 100nm and the islands did not merge. The nanoparticles were observed on the film, the density and the size of nanoparticles did not changes comparing with the sample grown at 1150'C. At lower temperature, 1050'C, the size of islands further decreased to 50nm. Comparing the contrast of islands, the islands became dark as the growth temperature decreases.

On exfoliated graphene, hBN film barely grows on the surface of graphite but it seems to be grown on the step edge of the flake. At 1150'C bright individual islands were sometime observed on the middle of the graphite film. Occasionally, bright lines were also observed on the surface. The diameter and the width of the islands and lines were about 200~400nm

respectively. Similar figures were obtained from the sample grown at the lower temperature; from the samples grown at 1100'C and 1050'C, only bright lines are observed from some region of flake. Interestingly, there was no nanostructure on the pristine graphite flake.

The hBN film grown on CVD multi-layer graphene and graphite flake with $O_2$ plasma treatment were characterized with Raman spectroscopy. For all samples, graphene peaks were dominantly observed; G-peak and 2D peak were observed around 1580cm$^{-1}$ and 2700cm$^{-1}$ respectively, proving that the $sp_2$ hybridized structure of graphene layers was maintained during the hBN growth.

In case of multi-layer graphene the shape of D-peak changed from single Lorentzian shape to a peak with shoulder. The center of peak shifted from 1363cm$^{-1}$ to 1373cm-1, supporting that the as-grown film is hBN which has a peak around 1367cm$^{-1}$ to 1373cm-1. However, the emergence of hBN peak cannot be clearly observed as the peak of hBN overlaps with the D-peak located around 1360cm$^{-1}$. On graphite flake with O2 plasma treatment, no significant change was observed in overall shape; G-peak and 2D-peak were observed in similar intensity regardless of the growth temperature and D-peak was not shown on the spectrum. On the region around 1370cm$^{-1}$, one peak appears at 1373cm$^{-1}$ as the growth temperature increases. Considering that the coverage of hBN film increases with increasing growth temperature, the peak which appears at 1373cm$^{-1}$ was originated from the grown film as the intensity of peak also increases with increasing growth temperature. Additionally, the position of peak implies that the film was hBN.

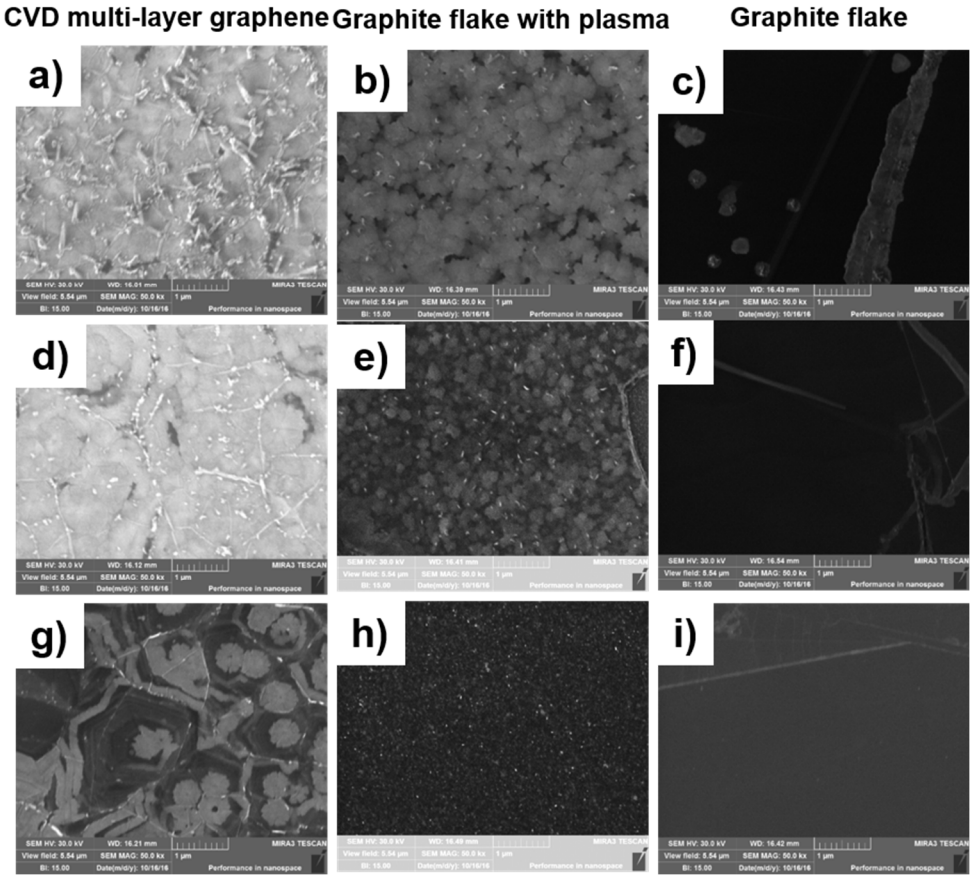


**Figure 4.1. FE-SEM images of hBN film grown on various graphene layers with different growth temperature.** hBN grown at (a-c) 1150'C, (d-f) 1100'C, (g-i) 1050'C.

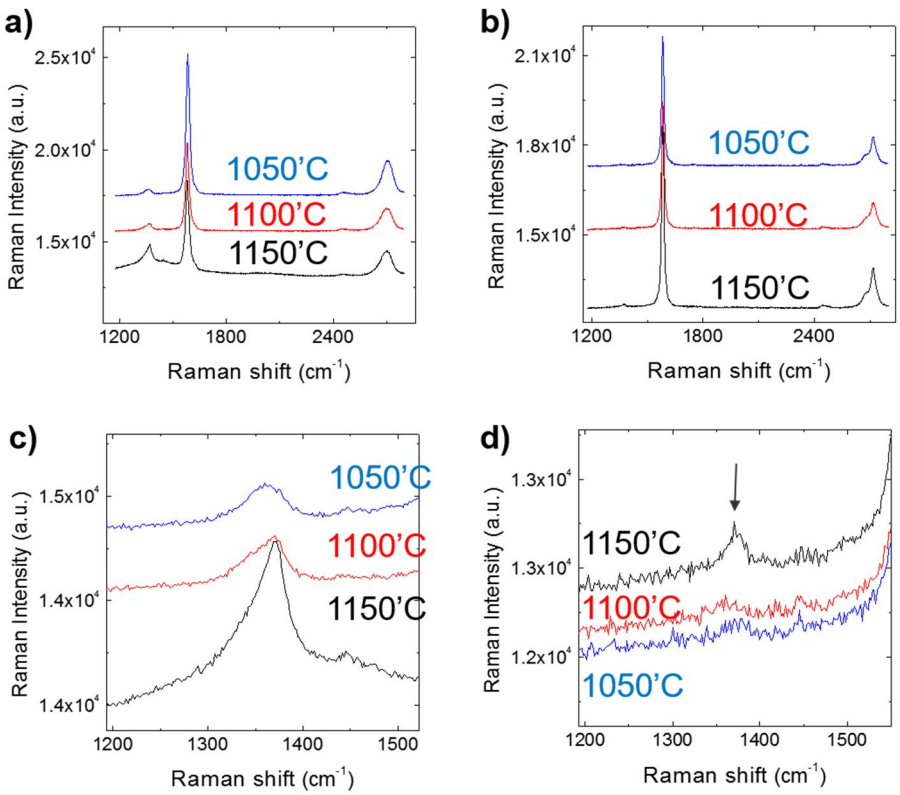


**Figure 4.2. Raman spectra of hBN film grown on graphene layers. Raman spectrum of hBN grown on** (a) CVD multi-layer graphene and (b) graphite flake with $O_2$ plasma treatment. (c, d) the magnified spectrum of (a) and (b)

## 4.2. Effect of pressure on hBN growth

The effect of pressure has been studied. hBN films were grown at various pressure of 150 − 650 torr. CVD graphene, graphite flake and graphite flake with O2 plasma treatment were used as substrates.

Figure4.3. shows FE-SEM images of hBN film grown on graphene films On CVD graphene, film-like feature was observed regardless of the growth pressure. At 150 torr, bright stripes and islands were grown on CVD graphene. Surface of the stripe and island looks flat. Nanoparticles or any other nanostructures were barely observed but the wrinkles of CVD graphene layer were observed. When the pressure increased to 300 torr, one complete film was synthesized. Some holes, particles and nanotubes were observed on the middle of the film. Although the contrast of the film was not perfectly uniform, the surface of the film seems flat. When the pressure was further increased to the 650 torr, film with increased density of nanostructure was grown on the CVD layers. Nanoneedles and particles were observed on the middle of the film while the density and the size of the structures were increased comparing with the sample grown at 300 torr.

On $O_2$ plasma treated graphite flake, growth of hBN film strongly depends on the growth pressure. When the pressure was low, only bright stripes were observed without any structure. As the pressure increased, the contrast of the film became bright and the nanoneedles were grown in addition to the islands. When the pressure was further increased, the islands merged into one complete film. Unlike the hBN film grown on CVD graphene, particles or nanoneedles were barely observed on the hBN film.

Although the density of nanostructure was greatly reduced as the growth pressure increases, pin holes were observed on the middle of the flake. On graphite flake without plasma treatment, only bright stripes were occasionally observed without any nanostructures.

Figure4.4. shows corresponding Raman spectrum of hBN film grown on graphene films. Raman spectrum of hBN film grown on CVD graphene and graphite flake with $O_2$ plasma treatment were obtained.

For all samples, graphene peaks were dominantly observed. In case of multi-layer graphene D-peak was observed around 1360$cm^{-1}$ in addition to G-peak and 2D peak. The shape of D-peak changed from single Lorentzian shape to peak without shoulder as the pressure increases. Additionally, the highest position of peak was shifted from 1360$cm^{-1}$ to 1370$cm^{-1}$, supports that the as grown film composed of the hBN which has Raman signal around 1367$cm^{-1}$ to 1373$cm^{-1}$ depending on the number of layers.

On graphite flake with O2 plasma treatment, G- and 2D peak were clearly observed without D-peak at 1360$cm^{-1}$. The intensity and position of G-peak and 2D-peak were same regardless of the growth pressure. When the growth pressure was 150 torr or 300 torr, no peak was observed around 1370cm-1. From the sample growth around 650 torr, small peak appeared at 1370cm-1, indicates that the film grown on graphene is hBN.

This results, the occurrence of hBN peak on Raman spectra, strongly support that the film grown on graphene composed of hBN.

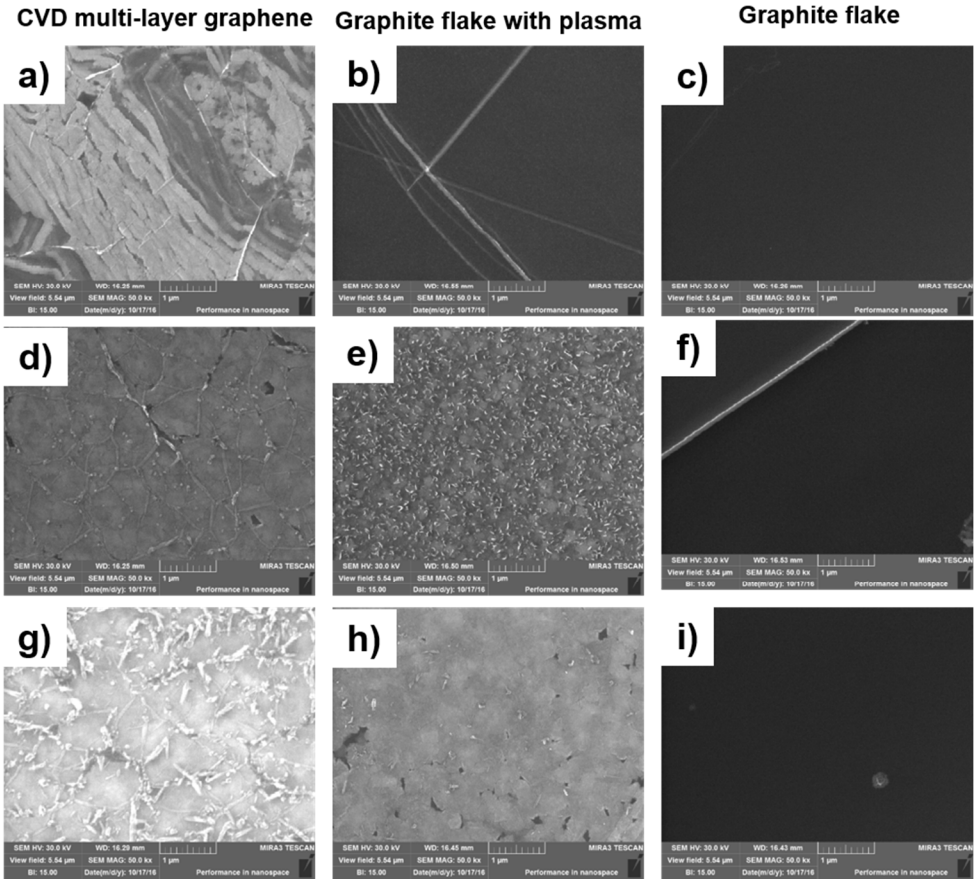


**Figure 4.3. FE-SEM images of hBN film grown on various graphene layers with pressure.** hBN grown at (a-c) 150 torr, (d-f) around 300 torr, and (g-i) around 650 torr.

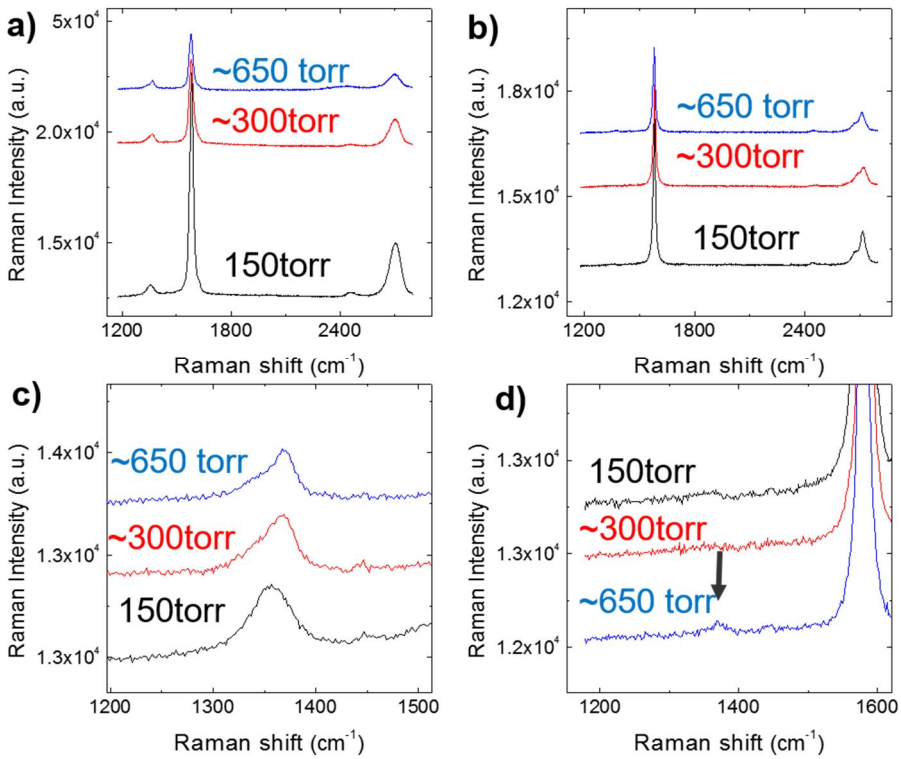


**Figure 4.4. Raman spectra of hBN film grown on graphene layers.** hBN film grown on (a) CVD multi-layer graphene and (b) graphite flake with O2 plasma treatment. (c, d) the magnified Raman spectra of (a) and (b)

## 4.3. Effect of borazine flowrate on hBN growth

In order to observe the effect of borazine flowrate on the growth of hBN film on graphene layers, hBN films have been grown with various borazine flowrate. hBN films were grown at various borazine flowrate from 6 sccm to 10 sccm. Graphite flake with $O_2$ plasma treatment and CVD multi-layer graphene were used as substrates.

Figure4.5. shows FE-SEM images of hBN film grown on various kinds of graphene films. On CVD multi-layer graphene, film-like feature was observed from all samples regardless of the borazine flowrate. When borazine flowrate was 6 sccm, graphene layers were mostly covered with newly grown hBN film. On the flat hBN film, particles and small nanoneedles were occasionally observed. The diameter of nanneedle is about 50~100nm. As flowrate of borazine was increased to 8 sccm, both density and size of nanostructure were significantly increased. Although flat film was observed on some region, the graphene layer was mostly covered with nanoneedle. The diameter of nanoneedle was increased to 100~200nm. Although the length of nanoneedle cannot be precisely estimated, the length of needles seems to be increased comparing to the needle grown with 6 sccm of borazine flowrate assuming that the needles were tiled with the same angles. When the flowrate of borazine was further increased to 10sccm, nanoneedles were more densely grown, and the film-like feature was barely observed. The size of nanostructure looks similar with the needles grown with 8 sccm, have diameter aound 100~200nm, while the nanoneedles densely grows and almost fully covers the film.

On oxygen plasma treat graphite, similar growth behavior was observed as it was on CVD graphene layers. When flowrate was 6 sccm, the graphite flake was mostly covered with hBN film. In addition to the film, nanostructures were grown on the film. The morphology of nanostructure seems like vertically standing nanosheets. Comparing with CVD MLG, nanostructures were evenly distributed over the substrate. When the flowrate of borazine was increased, same growth behavior was observed; the density and the size of nanostructure was increased and the morphology of nanostructure became nanoneedle. For flowrate of 8 sccm, nanoneedle with 50~100nm of diameters were observed. Unlike the CVD MLG case, surface of film was not flat but particles are densely distributed over the surface of film. When flowrate was 10 sccm, the diameter of nanoneedle was increased to 100~20nm, and particles were densely deposited on the surface of the film.

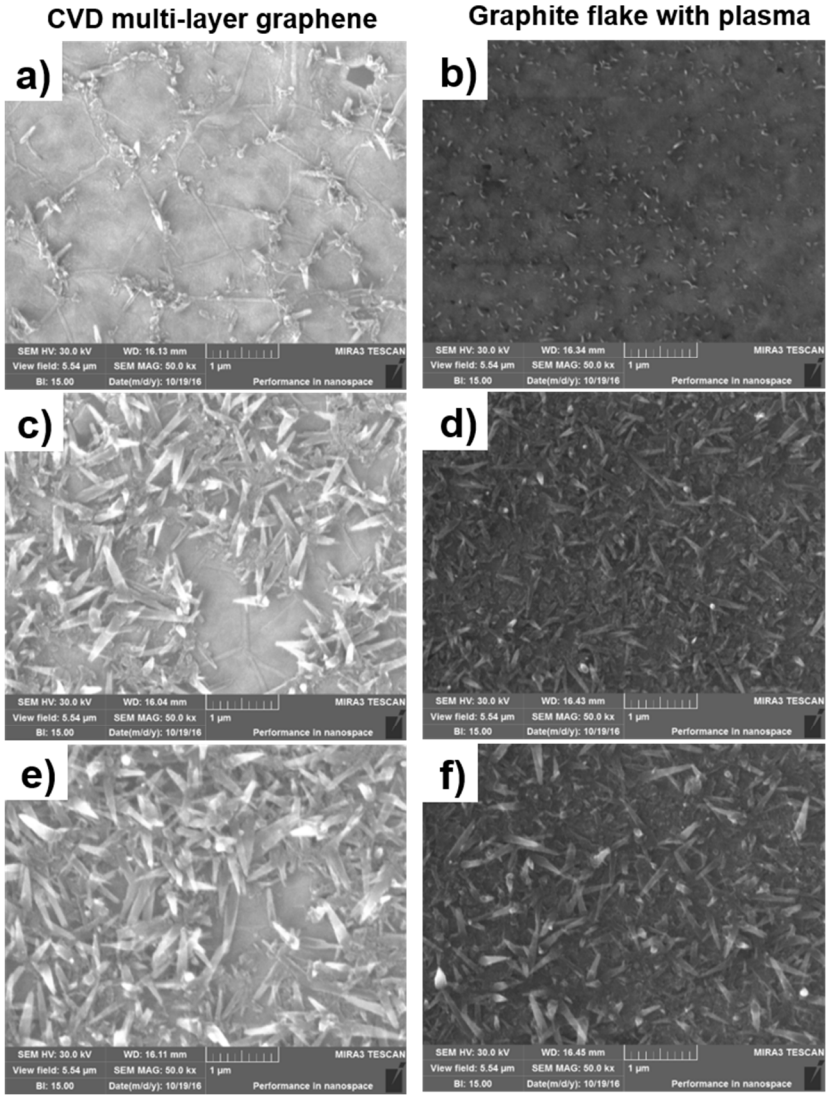


**Figure 4.5. FE-SEM images of hBN film grown on various graphene layers with different borazine flowrate.** hBN grown with (a-b) 6 sccm, (c-d) 8 sccm, and (e-f) 10 sccm of borazine flowrate.

## 4.4. Effect of growth time on hBN growth

To understand the growth behavior of hBN, growth time has been varied. From previous results, the film-like feature and nanostructures are both grown on graphene layers, and both features are observed simultaneously. For most cases, nanostructure and nanoneedles seem to be grown on hBN film, implying that the growth of nanostructure begins after the film covering the graphene layers. In order to confirm this growth behavior, growth time has been varied.

Figure4.6. shows the FE-SEM images of hBN grown on graphene layers. hBN film has been grown with various growth time of 15 minutes to 1 hour. CVD mutli-layer graphene and exfoliated graphite with $O_2$ plasma treatment were used as substrates.

When hBN had been grown for 15 minutes, small islands were grown on graphene layers and started to merge in to on complete film. On CVD multi-layer graphene, 200~400 nm size bright islands were grown and on some region, the islands were merged and forming big film. No nanostructures were observed on the surface of the film, and only wrinkles which might be originated from the underlying CVD graphene layers were observed. On exfoliated graphite with $O_2$ plasma treatment, 50~100nm size small islands were uniformly grown on the surface of graphite layer. Unlike the film grown on CVD graphene layers which started to merge, no film-like feature was observed. Additionally, No nanostructures were observed except the small islands.

When growth time was increased to 30 minutes, graphene layers were fully covered with hBN film and nanostructures were also grown on the hBN film. On CVD multi-layer graphene, hBN film with flat surface fully was grown on graphene layers. The surface of film looks flat except the nanostructures and wrinkle. In addition to the film, wrinkles were also observed which was observed from the hBN film grown for 15 minute. Nanostructures, which seems like nanoneedle, were also grown on the film. The size of nanostructure was smaller than 100 nm. On exfoliated graphite with $O_2$ plasma treatment, similar feature was observed as it was on CVD graphene layers. Most of graphite layer was covered with hBN film and small nanostructures were distributed on the surface of film. Unlike the CVD graphene, no wrinkles were observed. Interestingly, nanostructures were uniformly distributed on the surface of hBN film when it grew on graphite layers while it grew on the specific location, for example, along the wrinkle, on the CVD graphene layers.

When growth time was further increased to 1 hour, the size of nanostructure increased. On CVD graphene layers, nanoneedles are grown on the flat hBN film, the length of nanoneedle reached 500nm. Considering that the nanoneedles were observed from the top, the length of nanoneedle would be longer than 500nm. In addition to the nanoneedles, the film-like feature was also observed underneath the nanoneedles. This feature implies that the growth of nanoneedle was not randomly occurred on the surface of hBN film but on specific area.

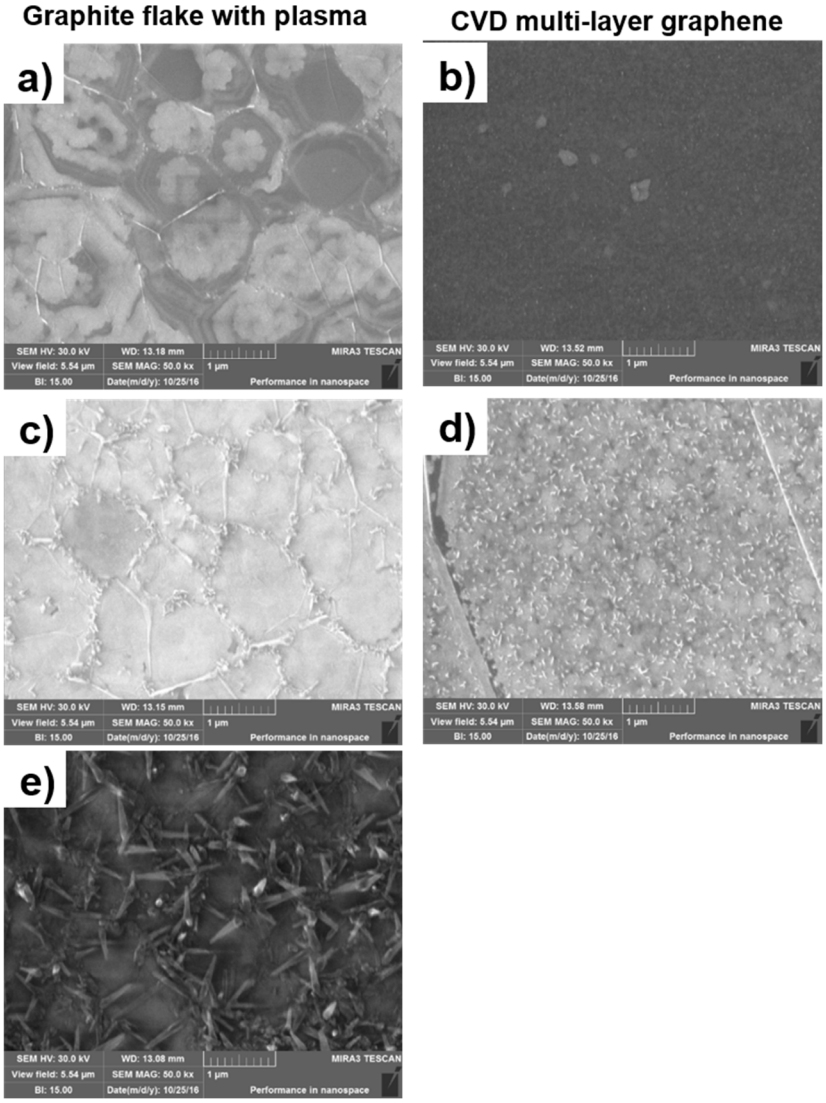


**Figure 4.6. FE-SEM images of hBN film grown on various graphene layers with different growth time.** hBN grown for (a-b) 15 minutes, (c-d) 30 minutes, and (e-f) 60 minutes.

## 4.5. Summary

The effects of growth conditions on the growth of hBN films on graphene layers have been studied on this chapter. hBN films and nanostructures were grown on the exfoliated graphite, graphite with $O_2$ plasma treatment and CVD multi-layer graphene while varying the growth temperature, pressure, flowrate of borazine and growth time. hBN islands were formed on graphene layers and merged into complete film depending on the growth temperature and pressure. It was confirmed by Raman spectroscopy that the grown film was hBN. In addition to the film, nanoneedles or nanoparticles were also formed on the surface of film. Varying the growth time, it was observed that the film firstly covered the graphene layers and additional nanostructures were grown on the film.

# Graphene growth on hBN layers

# 5

This chapter describes the growth of graphene on hBN layers under various growth conditions. The growth of graphene on hBN layer has been accomplished by several groups and it is known that the growth of graphene on hBN was realized at 1150'C with $H_2/CH_4$ ratio 50. Based on this conditions, the growth conditions of graphene on hBN has been studied using our setup while varying the growth conditions—growth temperature, pressure and flowrate of ethylene—and the effect of each parameter has been observed.

## 5.1. Effect of pressure on graphene growth

The effect of pressure on the growth of graphene on hBN layer has been studied. The growth pressure has been varied from 50 torr to 740 torr with other conditions fixed. hBN flakes exfoliated on $SiO_2/Si$ were used as substrates.

Figure5.1. shows the graphene islands grown on hBN flakes. When growth pressure was 50 torr, irregular pattern was observed on the hBN flake. This feature was also observed from the pristine hBN flake, and no significant change was observed after the growth process. When growth pressure increased to 300 Torr, grey dots and stripes were observed on the hBN flake. The diameter of dot and the width of stripe were about 50nm. Grey dots were randomly distributed over the hBN flake. When growth pressure was increased to 740 torr, the grey dots and stripes were still observed. The diameter of dots and the width of stripe increased to 100nm. When growth time was increased to 30 minute while maintaining the

growth pressure at 740 torr, the diameter of dots and the width of stripe was further increased to 300~400nm.

Raman spectroscopy has been conducted to confirm that the islands grown on hBN flake were graphene. The peaks originated from hBN and graphene were respectively indicated with red and black arrows. When growth pressure was low, strong hBN peak was observed with small peak around 1580cm$^{-1}$. This peak is expected as G-peak of graphene which locates around the 1580cm$^{-1}$. As the growth pressure increased to 300 torr, the intensity of peak at 1580cm$^{-1}$ increased and additional peak appeared around 1360cm$^{-1}$ which might be the D-peak of graphene. When the growth pressure was further increased to atmospheric pressure, no significant change was observed comparing with the sample grown at 300 torr. 2D peak located around 2700cm$^{-1}$ was observed when the growth time was increased from 10 minute to 30 minute maintaining the atmospheric pressure. The occurrence of G- and 2D-peak indicates that the material deposited on hBN flake is graphene.

Relating the FE-SEM images and Raman spectroscopy, one can conclude that the grey islands on hBN flake were graphene. The intensity of graphene peaks were also increased with increasing pressure and time, implies that the amounts of graphene was increased. In addition to the Raman intensity, the diameter of island was increased with increasing growth pressure and growth time, and this tendency agrees with that observed from Raman spectra. Therefore, the islands grown on hBN flake were graphene and it generated the Raman signals.

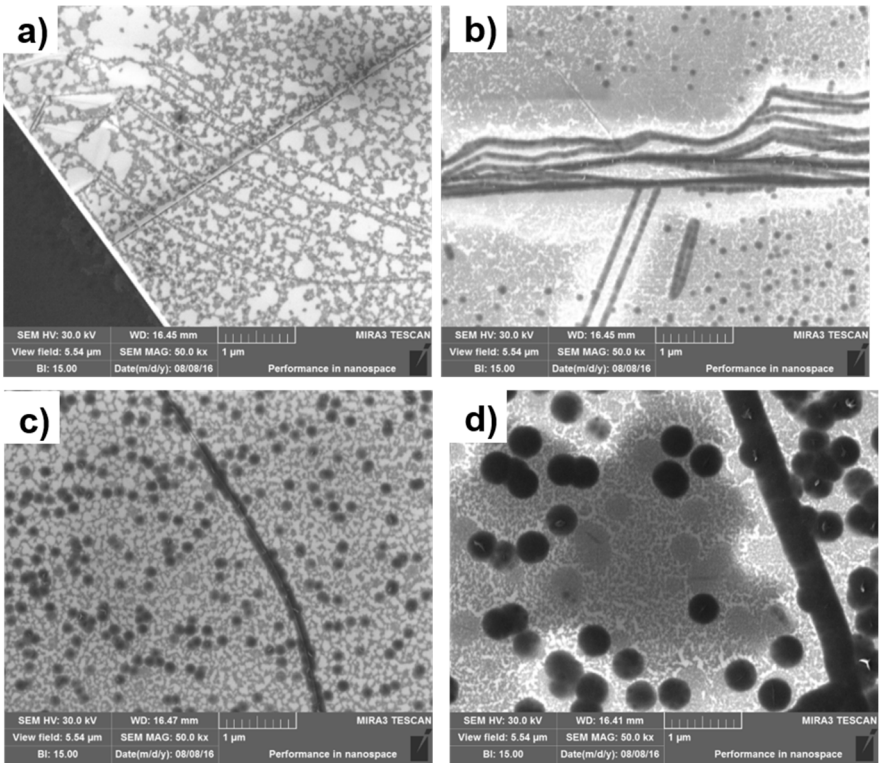


**Figure 5.1. FE-SEM images of graphene islands grown on hBN flakes with different pressure and growth time.** graphene was grown for 10 minutes under (a) 50 torr, (b) 300 torr and (c) 740 torr. (d) Graphene was grown for 30 minutes under 740 torr.

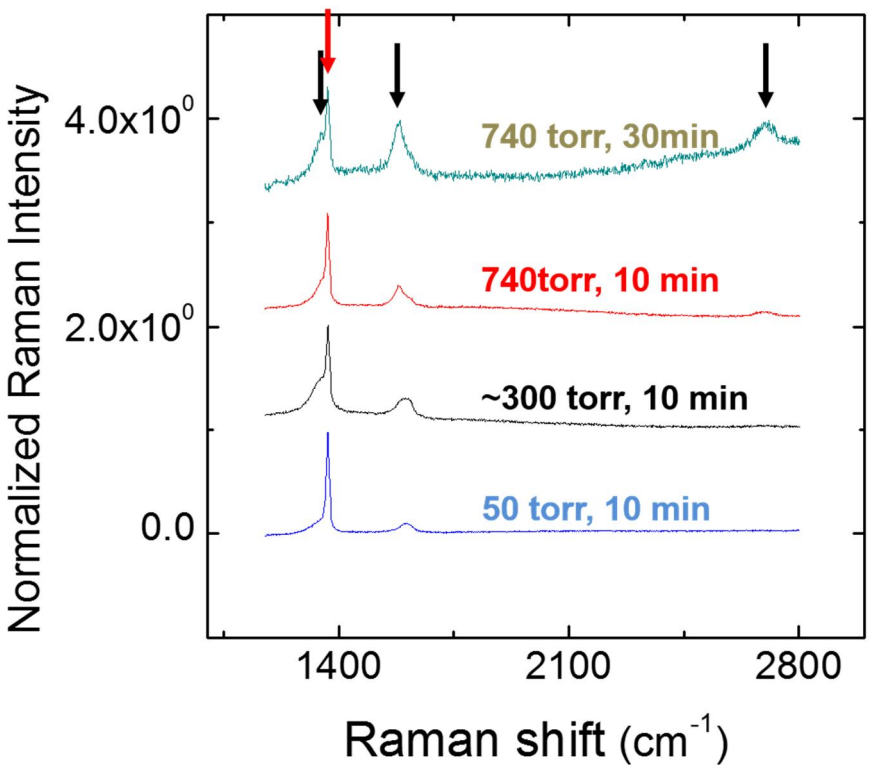


**Figure 5.2. Raman spectra of graphene grown under different pressure and growth time.** Black and red arrows indicates the Raman peaks of graphene and hBN respectively. To compare the spectra, intensity of spectra was normalized and vertically shifted.

## 5.2. Effect of temperature on graphene growth

The effect of temperature on the growth of graphene has been studied. Growth temperature was changed from 1000'C to 1200'C while maintaining the other growth conditions fixed. Growth pressure was controlled to be atmospheric pressure and growth time was 30 minutes.

When growth temperature was 1000'C, black islands and stripes were observed on the hBN flake. hBN flake was observed as bright region on SiO2/Si substrate and 100nm size graphene islands and stripes were observed. The stripes were formed because the graphene nucleated preferably on the stepedge of underlying hBN flake. When characterized with Raman spectroscopy, small G-peak was observed at 1600cm$^{-1}$ in addition to the strong hBN peak at 1367cm-1, confirms that the islands were composed of graphene. When growth time was increased to 1100'C, the size and density of graphene islands were increased. The size of graphene islands was about 200 nm, and the underlying hBN film was mostly covered by the graphene islands. On the Raman spectrum, the graphene peaks—D-, G-, and 2D- peaks—were all observed and the intensity of graphene peak was comparable to the hBN peak, indicates that the amounts of graphene was increased. As the growth temperature was further increased to 1200'C, growth behavior was changed. hBN flake was fully covered by graphene islands. 3-dimensional nanoparticles were also observed in addition to the islands when graphene was grown at 1200'C. On Raman spectrum, the intensity of graphene peaks was increased and no hBN peak was observed in this case.

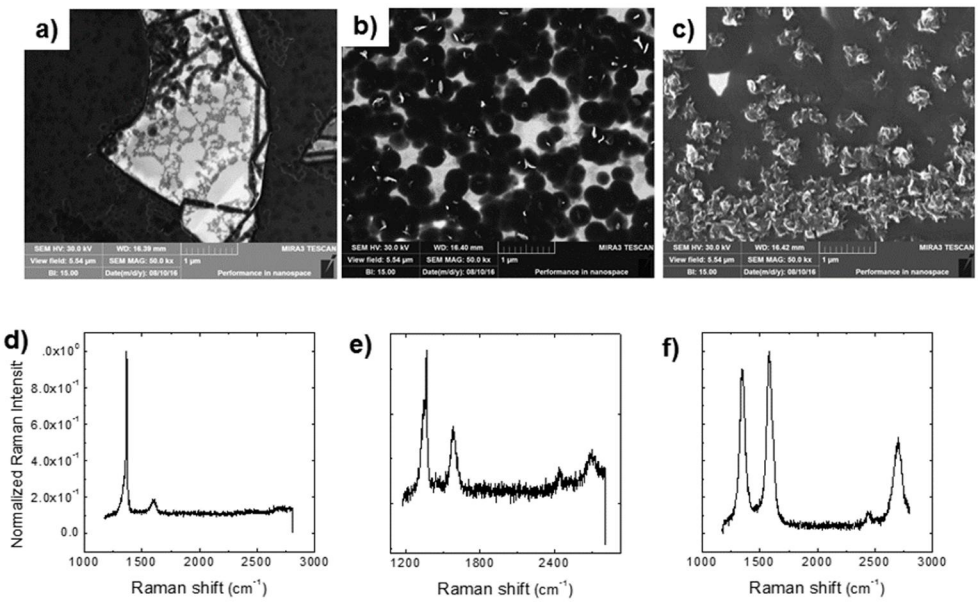


**Figure 5.3. FE-SEM images and corresponding Raman spectra of graphene grown on hBN flakes with growth temperature.** Graphene was grown at (a) 1000'C (b) 1100'C and (c) 1150'C. (d-f) corresponding Raman spectrum of graphene grown on hBN.

## 5.3. Effect of ethylene flowrate on graphene growth

To study the effect of ratio between carbon source and hydrogen, the flowrate of ethylene has been changed. Since the hydrogen atmosphere known to decompose the amorphous carbon deposited in addition to the graphene layers, the ratio between carbon and hydrogen is very important in synthesizing high quality graphene.

The flowrate of ethylene has been changed from 50 sccm to 200 sccm while maintaining the other conditions fixed. The Figure5.4. shows the FE-SEM images of graphene islands grown on pristine hBN flakes. When flowrate was 50 sccm, 100~200nm size islands were observed on the hBN flake. As pointed with red arrows, hexagonal islands were observed and these islands seems to be aligned on specific direction. This alignment implies that the graphene islands have epitaxial relation with underlying hBN flake. When flowrate was increased to 100 sccm, the diameter of islands increased to 300~400 nm and the islands have circular shape, not hexagonal. On the middle of some islands, small 3-dimensional nanostructures were observed. In addition to the change on the shape of islands, the density of island was increased, the coverage of graphene was increased comparing with the sample grown with 50 sccm of ethylene. When flowrate was further increased to 150 and 200 sccm, hBN flake was mostly covered with graphene islands and the nanostructures on it. On the black graphene islands, nanostructures, which looks like crumpled nanosheets, were observed.

This results implies that 50 sccm of flowrate is proper in synthesizing high quality graphene in 2-dimensional form without amorphous carbon.

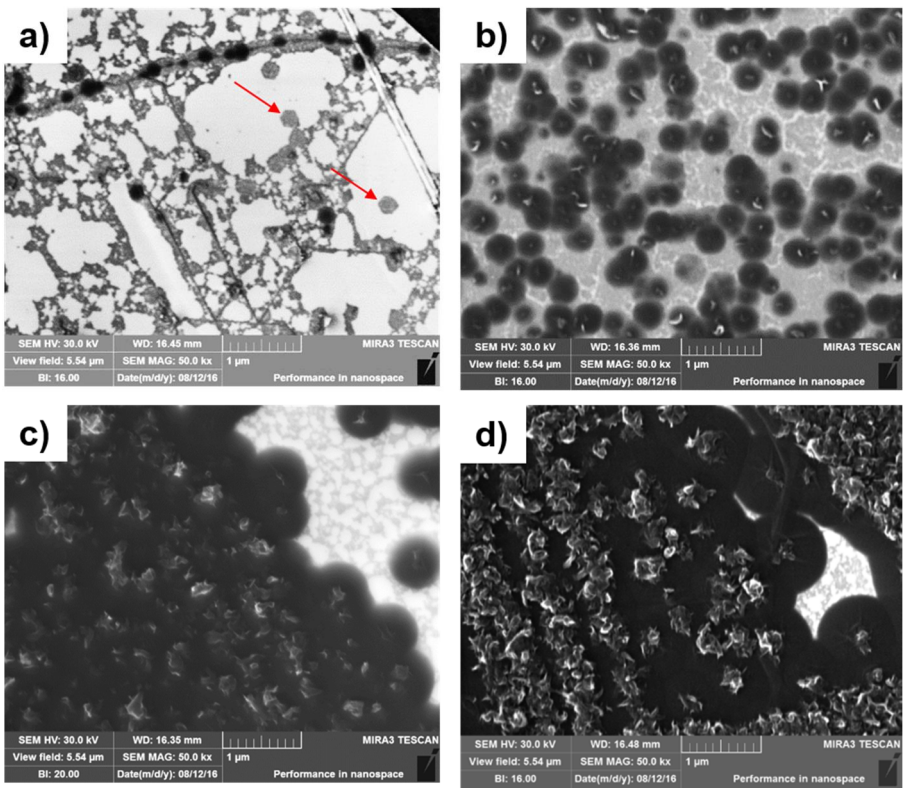


**Figure 5.4. FE-SEM images graphene grown on hBN flake with different ethylene flowrate.** Graphene was grown with (a) 50 sccm ,(b) 100sccm (c) 150 sccm, and (d) 200 sccm of ethylene. The red arrows indicates the graphene islands with hexagonal shape

## 5.4. Summary

The effects of growth conditions on the growth of graphene on hBN have been studied on this chapter. Graphene islands and 3-dimensional nanostructures were grown on the exfoliated hBN while varying the growth temperature, pressure and flowrate of ethylene. Graphene islands were formed on hBN layers and nanostructures were grown on graphene islands depending on the growth temperature, pressure and the amounts of ethylene. It was confirmed by Raman spectroscopy that the grown film was graphene. On specific growth conditions, hexagonal islands aligned in specific direction was observed, implies the epitaxial growth of graphene on hBN layers.

# Sequential growth of hBN and graphene on hBN layers

# 6

This chapter describes the growth of hBN and graphene hetrostructures. When graphene and hBN can be grown with no use of catalyst, the thickness or quality of underlying film does not matter but only surface of film would affect the growth behavior. It implies that graphene and hBN vertical heterostructure or superlattice can be obtained just by sequentially growing the graphene and hBN. In order to confirm this hypothesis, graphene and hBN have been sequentially grown on the same substrate and characterized.

## 6.1. Sequential growth of graphene and hBN

Figure6.1. shows the schematic of growth process. Firstly, exfoliated hBN flakes were prepared on $SiO_2$/Si substrates. Graphene was grown on hBN flakes using the previously developed growth conditions; at 1150˚C under atmospheric pressure, growth was done for 30 minutes while introducing the 50 and 2600 sccm of ethylene and hydrogen respectively. After the graphene growth, the susceptor was cooled down until the temperature reaches around 100˚C. When the susceptor was fully cooled down, in-situ growth of hBN was done; at 1150˚C under 600 torr, growth was carried out for 30 minutes. If as-grown graphene and hBN were vertically stacked, the graphene layer might be encapsulated with hBN layer as shown on the figure.

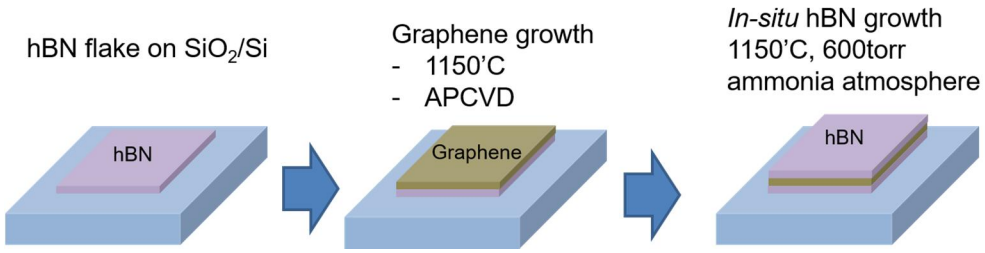


**Figure 6.1. Schematics of experiment. Sequential growth of graphene and hBN on hBN flakes**

## 6.2. FE-SEM images and Raman spectrum of the film

After the sequential growth of graphene and hBN, the samples were characterized with FE-SEM and Raman spectroscopy. Pristine hBN flakes and oxidized hBN flakes were used as substrates.

Figure6.2. shows the FE-SEM images of film after the sequential growth on hBN flakes. On both substrates, some materials seem to be deposited on the hBN flakes. On pristine hBN flake, islands of 300~400 nm diameter were distributed over the surface of hBN flakes, and the other area has non-uniform darker contrast comparing with the contrast of islands. Some islands seem to be merged and began to form larger islands. Needle-like nanostructures were observed on the surface of islands. On hBN flake oxidized at 900'C for 3 hours, islands were more densely grown comparing to the pristine hBN flakes, and almost merged into one complete film. Nanoneedles which were similar to the needles observed on pristine hBN flake were observed on the surface of the film. Unlike the film grown on pristine hBN flake, the area between each islands were almost filled, not showing abrupt changes on the contrast.

Characterizing with Raman spectroscopy, graphene and hBN peaks were observed from both samples. From the film grown on pristine hBN flake, both graphene and hBN peaks were clearly observed, and two signals have comparable intensity. Broad D-peak overlapped with sharp hBN peak around 1360$cm^{-1}$, and G- and 2D-peak were observed at 1573 $cm^{-1}$ and 2682 $cm^{-1}$ respectively. From the film grown on oxidized hBN flake, sharp hBN peak was clearly observed while the graphene peaks were barely observable because of the small intensity. Considering

that hBN film grown on graphite layers makes both hBN and graphene peaks on the spectrum, the small graphene peak might indicate the absence of graphene underneath hBN layers. Additionally, it cannot be confirmed whether as the film covering the surface of flake is hBN or not because the hBN peak on the spectrum can be originated from underlying hBN flake.

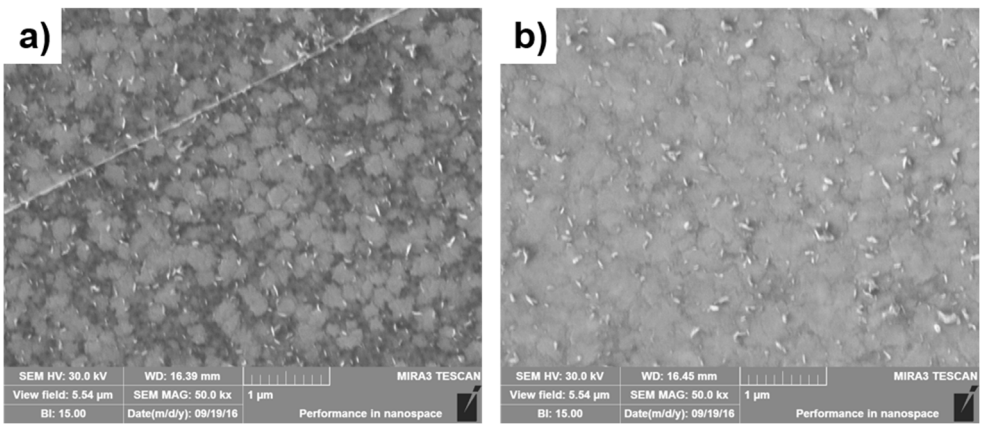


**Figure 6.2. FE-SEM images of film after the sequential growth**. a) On pristine hBN flake, b) On hBN flake oxidized under 900'C for 3 hours

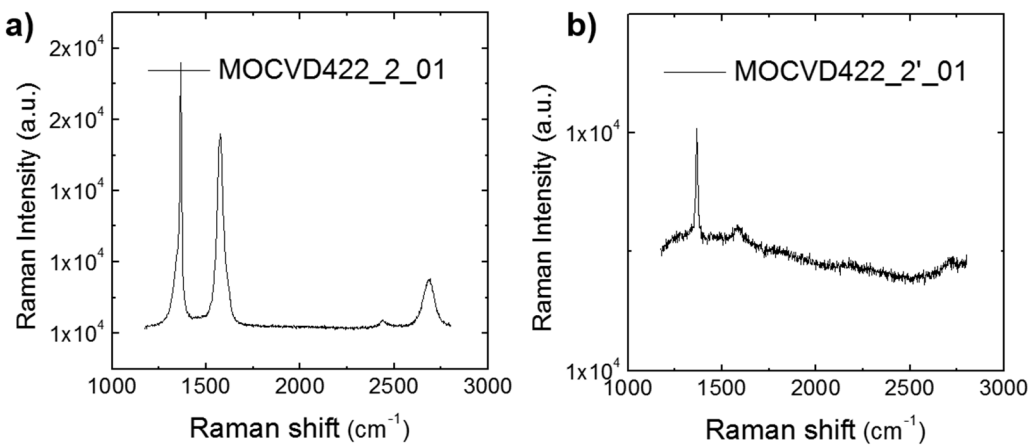


**Figure 6.3. Raman spectrum of the film after the sequential growth**. Spectrum obtained from a) pristine hBN flake and b) oxidized hBN flake

## 6.3. Microstructure of hBN/graphene grown on hBN flakes

Microstructure of the film grown on oxidized hBN flakes were characterized with high-resolution transmission electron microscope(HR-TEM). Observing the surface of the film. Highly periodic arrays were observed on some region. The distance among two bright spots was 2.50A, precisely matches with the lattice constant of hBN in direction of (101bar0) plane. Corresponding FFT image shows six fold symmetry, indicating the arrays were highly periodic and having six fold symmetry. Considering that the HR-TEM gives highly precise value concerning lattice constant, this two results indicate that the surface of film consists of hBN, not graphene as graphene has smaller lattice constant comparing with hBN.

Observing the sample with low magnification image, there are some region with regular patterns on it pointed with red arrow. Obtaining high resolution images from those areas, we can see the highly ordered pattern. Measuring the intensity of the images along one line, I observed that the bright spot is aligned with the period 2.50 A. Performing the FFT on this image six fold symmetry is observed.

These two feature, the period and symmetry perfectly matches with that of BN, so this results indicates that the surface of sample is covered with hBN.

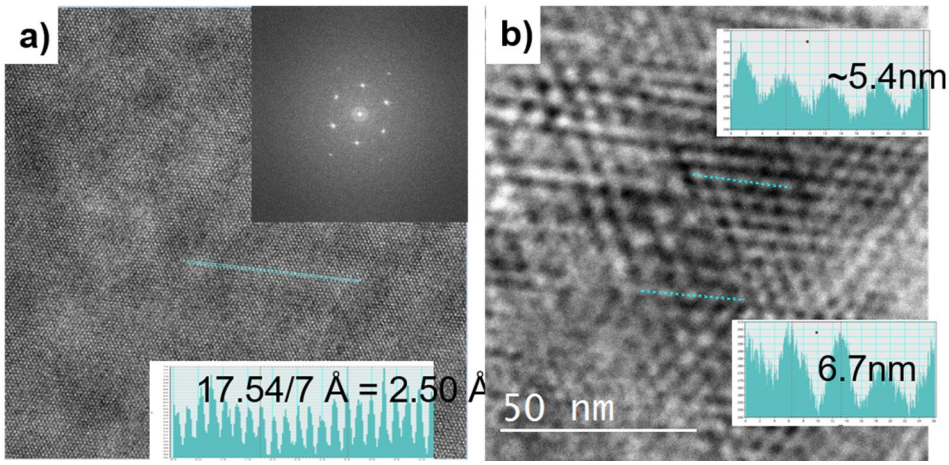


**Figure 6.4. High resolution TEM images of film grown on hBN flake after the sequential growth.** a) High resolution TEM image and corresponding FFT image(inset) b) Low magnification TEM image showing Moire pattern

## 6.4. Summary

This chapter describes a sequential growth of graphene and hBN on hBN flakes. Based on the growth condition developed on previous chapters, graphene and hBN were in-situ grown on hBN flakes. FE-SEM images confirmed that newly grown film covered the original hBN flakes, and Raman spectroscopy and TEM analysis indicates that both graphene and hBN was grown on the film. The structure of film was not fully understand whether graphene and hBN was vertically stacked or not.

# Conclusion

# 7

## 7.1. Summary

The goal of this research was to provide a new growth technique for the facile growth of graphene and hBN heterostructures or supperlattices and shows potential of growing heterostructure of arbitrary 2D materials. Growth of graphene, hBN and their heterostructure have been demonstrated and the effect of growth conditions have been studied using CVD setup. Based on the growth conditions developed for graphene and hBN growth, the growth of vertical heterostructures of graphene and hBN has been attempted by sequential growth of graphene and hBN.

# Reference


1. Banszerus, L., et al., Ultrahigh-mobility graphene devices from chemical vapor deposition on reusable copper. Sci Adv, 2015. **1**(6): p. e1500222.

2. Fan, Y., et al., Crack-Free Growth and Transfer of Continuous Monolayer Graphene Grown on Melted Copper. Chemistry of Materials, 2014. **26**(17): p. 4984-4991.

3. Li, X., et al., Large-area synthesis of high-quality and uniform graphene films on copper foils. Science, 2009. **324**(5932): p. 1312-4.

4. Reina, A., et al., Growth of large-area single- and Bi-layer graphene by controlled carbon precipitation on polycrystalline Ni surfaces. Nano Research, 2010. **2**(6): p. 509-516.

5. Wang, J., et al., High-mobility graphene on liquid p-block elements by ultra-low-loss CVD growth. Sci Rep, 2013. **3**: p. 2670.

6. Zou, Z., et al., Uniform single-layer graphene growth on recyclable tungsten foils. Nano Research, 2015. **8**(2): p. 592-599.

7. Bae, S., et al., Roll-to-roll production of 30-inch graphene films for transparent electrodes. Nature Nanotechnology, 2010. **5**(8): p. 574-578.

8. Kobayashi, T., et al., Production of a 100-m-long high-quality graphene transparent conductive film by roll-to-roll chemical vapor deposition and transfer process. Applied Physics Letters, 2013. **102**(2): p. 023112.

9. Wu, T., et al., Fast growth of inch-sized single-crystalline graphene from a controlled single nucleus on Cu-Ni alloys. Nat Mater, 2016. **15**(1): p. 43-7.

10. Zhou, H., et al., Chemical vapour deposition growth of large single crystals of monolayer and bilayer graphene. Nat Commun, 2013. **4**: p. 2096.

11. Petrone, N., et al., Chemical vapor deposition-derived graphene with electrical performance of exfoliated graphene. Nano Lett, 2012. **12**(6): p. 2751-6.

12. Kim, G., et al., Growth of high-crystalline, single-layer hexagonal boron nitride on recyclable platinum foil. Nano Lett, 2013. **13**(4): p. 1834-9.

13. Kim, K.K., et al., Synthesis and Characterization of Hexagonal Boron Nitride Film as a Dielectric Layer for Graphene Devices. Acs Nano, 2012. **6**(10): p. 8583-8590.

14. Lee, K.H., et al., Large-scale synthesis of high-quality hexagonal boron nitride nanosheets for large-area graphene electronics. Nano Lett, 2012. **12**(2): p. 714-8.

15. Shi, Y., et al., Synthesis of few-layer hexagonal boron nitride thin film by chemical vapor deposition. Nano Lett, 2010. **10**(10): p. 4134-9.

16. Song, L., et al., Large scale growth and characterization of atomic hexagonal boron nitride layers. Nano Lett, 2010. **10**(8): p. 3209-15.

17. Tay, R.Y., et al., Growth of large single-crystalline two-dimensional boron nitride hexagons on electropolished copper. Nano Lett, 2014. **14**(2): p. 839-46.

18. Gao, Y., et al., Repeated and Controlled Growth of Monolayer, Bilayer and Few-Layer Hexagonal Boron Nitride on Pt Foils. Acs Nano, 2013. **7**(6): p. 5199-5206.

19. Lupina, G., et al., Residual Metallic Contamination of Transferred Chemical Vapor Deposited Graphene. Acs Nano, 2015. **9**(5): p. 4776-4785.

20. Lin, Y.C., et al., Graphene annealing: how clean can it be? Nano

Lett, 2012. **12**(1): p. 414-9.

21. Liu, N., et al., The origin of wrinkles on transferred graphene. Nano Research, 2011. **4**(10): p. 996-1004.

22. Wang, M., et al., Catalytic Transparency of Hexagonal Boron Nitride on Copper for Chemical Vapor Deposition Growth of Large-Area and High-Quality Graphene (vol 8, pg 5478, 2014). Acs Nano, 2014. **8**(8): p. 8711-8711.

23. Wu, Q., et al., In situ synthesis of a large area boron nitride/graphene monolayer/boron nitride film by chemical vapor deposition. Nanoscale, 2015. **7**(17): p. 7574-9.

24. Tay, R.Y., et al., Direct growth of nanocrystalline hexagonal boron nitride films on dielectric substrates. Applied Physics Letters, 2015. **106**(10): p. 101901.

25. Kobayashi, Y. and T. Akasaka, Hexagonal BN epitaxial growth on (0001) sapphire substrate by MOVPE. Journal of Crystal Growth, 2008. **310**(23): p. 5044-5047.

26. Kobayashi, Y., T. Akasaka, and T. Makimoto, Hexagonal boron nitride grown by MOVPE. Journal of Crystal Growth, 2008. **310**(23): p. 5048-5052.

27. Ding, X., et al., Direct growth of few layer graphene on hexagonal boron nitride by chemical vapor deposition. Carbon, 2011. **49**(7): p. 2522-2525.

28. Mishra, N., et al., Rapid and catalyst-free van der Waals epitaxy of graphene on hexagonal boron nitride. Carbon, 2016. **96**: p. 497-502.

29. Son, M., et al., Direct growth of graphene pad on exfoliated hexagonal boron nitride surface. Nanoscale, 2011. **3**(8): p. 3089-93.

30. Tang, S., et al., Nucleation and growth of single crystal graphene on hexagonal boron nitride. Carbon, 2012. **50**(1): p. 329-331.

31. Tang, S., et al., Precisely aligned graphene grown on hexagonal boron nitride by catalyst free chemical vapor deposition. Sci Rep, 2013. **3**: p. 2666.

32. Yang, W., et al., Epitaxial growth of single-domain graphene on hexagonal boron nitride. Nat Mater, 2013. **12**(9): p. 792-7.

33. Jang, A.R., et al., Wafer-Scale and Wrinkle-Free Epitaxial Growth of Single-Orientated Multilayer Hexagonal Boron Nitride on Sapphire. Nano Lett, 2016. **16**(5): p. 3360-6.

34. Lee, K.H., et al., Nanocrystalline-graphene-tailored hexagonal boron nitride thin films. Angew Chem Int Ed Engl, 2014. **53**(43): p. 11493-7.

35. Cho, Y.J., et al., Hexagonal Boron Nitride Tunnel Barriers Grown on Graphite by High Temperature Molecular Beam Epitaxy. Sci Rep, 2016. **6**: p. 34474.

# Summary in Korean

# 국문 요약문

그래핀의 발견 이후 2차원 물질을 이용한 새로운 구조의 소재와 소자에 대한 연구가 많이 진행되었다. 물리적으로 박리된 2차원 물질을 이용하여 그래핀이나 질화붕소와 같은 2차원 물질의 이종구조를 만들어 새로운 소재를 만들거나 소재의 특성을 관찰할 수 있었지만 이러한 소재를 대면적으로 만드는 방법에 대한 연구는 소재 특성에 대한 연구에 비해 부진한 상태이다. 금속 촉매나 실리콘 산화막 위에 단일 2차원 물질이나 2개 물질의 이종구조를 합성에 대한 연구들은 보고되었지만 물리적으로 박리된 2차원물질을 이용해 만든 소재와 같이 수 층의 2차원 물질을 쌓은 구조를 만드는 방법은 전혀 보고된 바 없다. 수 층이 겹겹이 쌓인 이종구조를 합성하기 위해서는 본 논문에서는 비촉매 화학기상증착법을 이용해 그래핀과 질화붕소를 합성하여 그래핀과 질화붕소의 종방향 이종구조를 합성할 수 있음을 보이고, 그래핀과 질화붕소를 순차적으로 합성하여 질화붕소-그래핀-질화붕소 구조를 제조할 수 있음을 보이고자 하였다. 그래핀과 질화붕소 사이의 에피탁시 관계를 이용하여 그래핀층 위에 질화붕소를, 질화붕소층 위에 그래핀 층을 합성하였고, 두 합성법을 이용하여 질화붕소층 위에 그래핀-질화붕소층을 순차적으로 합성하여 질화붕소-그래핀-질화붕소 구조를 합성하려 하였다. 또한, 이러한 구조를 화학기상증착법으로 합성할 수 있음을 보임으로써 2차원 물질의 수직이종구조의 대면적 합성이 가능함을 증명하고자 하였다.

주요어 : 비촉매 화학기상증착법, 그래핀, 육각질화붕소, 이종구조

학번 : 2015-20341